Analyst

Accepted Manuscript

ROYAL SOCIETY OF CHEMISTRY

www.rsc.org/analyst

CREATED USING THE RSC ARTICLE TEMPLATE (VER. 3.1) - SEE WWW.RSC.ORG/ELECTRONICFILES FOR DETAILS

Analyst www.rsc.org/xxxxxx | PAPER

Tethering of spherical DOTAP liposome gold nanoparticles on cysteamine monolayer for sensitive label free electrochemical detection of DNA and transfection

Mohanlal Bhuvana and Venkataraman Dharuman

Received (in XXX, XXX) Xth XXXXXXXXX 20XX, Accepted Xth XXXXXXXXX 20XX
DOI: 10.1039/b000000x

Construction of spherical liposome is critical for developing tools for targeted gene and drug delivery applications in biotechnology and medicine, however, demonstrated only in solution phase till now. Spherical liposome tethering on pristine thiol monolayer on gold transducer and its application to label free DNA sensing and transfection is rarely been reported. Here, we report tethering of spherical 1, 2-dioleoyltrimethylammoniumpropane liposome-gold nanoparticle (DOTAP-AuNP) on amine terminated monolayer by simple electrostatic interaction on gold transducer for the first time. Cuddling of cationic liposome by AuNP prevents the spherical vesicle fusion in both liquid and solid phases, an essential criterion required for gene and drug delivery applications. The spherical nature of DOTAP-AuNPs on gold surface is confirmed electrochemically using both $[Fe(CN)_6]^{3-/4-}$ and $[Ru(NH_3)_6]^{3+}$ redox probes. Atomic Force Microscopy (AFM), Fourier Transform Infrared Spectroscopy (FTIR), Transmission Electron Microscopy (TEM), Dynamic Light Scattering (DLS) and Ultraviolet – Visible (UV) spectroscopic techniques confirm the robust nature of spherical liposome-AuNPs on solid and in liquid phases. The surface is applied for label free DNA hybridization and single nucleotide polymorphism detections sensitively and selectively without signal amplification. The lowest target DNA concentration detected is 100 attomole. DNA transfection is made simply by dropping *E. coli* cells on DOTAP-AuNP-DNA immobilized transducer surface. Difference between Fluorescent image of the for transfected *E. coli* and the Differential Interference contrast image of *E.coli* cells by Confocal Laser Scanning Microscopy (CLSM) confirms the efficiency and simplicity of the transfection method developed in terms of reduced cost and reagents.

Keywords: Spherical, DOTAP, gold electrode, monolayer, DNA sensing, transfection

Introduction

Liposomes are effective platform being used for delivering small molecules, drugs, genes, imaging agents and nano particles and hence become hot spot for the past two decades in the field of chemistry and medical biology[1-7] An individual liposome can accommodate from zeptolitres (10^{-21}L) to femtolitres (10^{-15}L) of target analyte of our interest.[8]

Cationic liposomes with neutral lipids are widely used for transfection studies due to their higher transfection efficiency [9-17] less toxic,[18,19] non-immunogenic, non-inflammatory, biocompatible, biodegradable, ease of control over size and surface functionalization [20] compared to other conventional transfection methods that include calcium-phosphate precipitation, electroporation, detergent-DNA complexes, DNA-DEAE complexes, microinjection, virus-mediated transfection, and particle bombardment. Cationic liposomes are applied for variety of non-viral gene transfer.[21,22] It may be noted that the physical properties such as charge of liposome,[23] formulation of cationic and helper

Molecular Electronics Laboratory, Department of Bioelectronics and Biosensors, Science Block, Alagappa University, Karaikudi – 630 004 India.

**To whom correspondence should be addressed. V. Dharuman, E-mail: dharumanudhay@yahoo.com Phone: 91-4565-226385 Fax: 91-4565-225202*
Electronic Supplementary Information FTIR, UV, CV, EIS, DPV are available:. See DOI: 10.1039/b000000x

lipids, [24] metal cations [25] liposome to DNA concentration ratio [26] complexes and cell types have greater influence on gene delivery or gene expression.[27] Importantly, efficiency of gene transfection rely on the formation of stable spherical liposomes and protecting from their degradation essentially required for targeted gene therapy and drug delivery applications. Since the non-functionalized liposomes are less stable, AuNPs,[28-34] silica nano particles[35] and polymers[36,37] are being employed to stabilize liposomes against fusion and to enhance the transfection efficiency. Studies of liposomes on solid surfaces like metal oxides (SiO_2,[38] glass,[39] and TiO_2.[40-47]) and metals (Pt,[48] Hg,[47,49] Au[50, 51] and carbon[52]) indicate rupturing of spherical liposome, due to their high fluidity nature to form bilayer whose structure strongly depends on the lipid composition, the nature of the surface, temperature, ionic strength, and pH.[53] It is to note that the multifunctional colloidal spheres constructed by integrating different nano particles into one system, have greater control over surface chemistry that is useful for self-assembling process. [54-56]

Molecular layer like mercapto propinic acid supported spherical liposome is constructed on gold coated quartz crystal surface. [57-60] But not applied for label free DNA sensing and transfection. Intact spherical liposomes architectured on the solid surfaces by lithographic technique[60-63] and polymers.[64,65] Apart from their expensive and tedious protocol, these liposomes are not applied for DNA sensing and gene transfer. DNA functionalized liposome, streptAvidine and biotin[66] labelled DNA target interactions have been used for constructing DNA-directed liposomal assembly on gold surface for enzyme catalysis based DNA sensing,[67-72] which showed the lowest DNA detection limit of 5 $\times 10^{-14}$ M by electrochemical method. This sensitivity is comparable with other conventional optical techniques such as fluorescence and surface plasmon resonance.[73,74] But the optical methods have limitation to develop low cost, miniaturized and portable devices for onsite or field analysis. Hence, development of electrochemical sensor platforms and devices are required for DNA sensing and transfection. In this context, self-assembled monolayer based DNA sensor on gold transducer[75,76] showed only picomolar concentration (1×10^{-12} M) detection limit by label free detection method. Therfore, the use of spherical liposome and AuNP nano composite supported by self-assembled monolayer could improve detection limit and sensitivity further.

Immobilization of the spherical liposome stabilized by AuNP supported by thiol monolayers on gold surface is rarely reported for DNA sensing and transfection in the literature even though it is simple, provides better control of surface chemistry and inexpensive than the other methods reported. Here, we constructed a spherical DOTAP stabilized by AuNP in buffer solution and immobilized on the amine terminated cysteamine monolayer on gold disc electrode by simple electrostatic interaction for the first time. High stablility and sensitivity of the DOTAP-AuNP on the electrode surface is indicated by the lowest detection limit (attomole concentration range) in presence of $[Fe(CN)_6]^{3-/4-}$. The used synthetic DNA sequence corresponds to *E. coli* cells. Following this, *E. coli* cells are transfected just by incubation in presence of DNA intercalator ethidium bromide (EtBr). The electrochemical behavior of the spherical DOTAP-AuNP on the cysteamine monolayer and label free DNA sensing are analyzed using Cyclic Voltammetry (CV) and Electrochemical Impedance Spectroscopy (EIS) methods. AFM, TEM, DLS, UV-Vis and FTIR techniques are used to explore the stability and interactions between the DOTAP, AuNPs and DNA. The gene transfer in *E. coli* cell is monitored by Confocal Laser Scanning Microscopy (CLSM).

Experimental Section

Materials

Potassium ferrocyanide, potassium ferricyanide, sulfuric acid, hydrogen peroxide, sodium chloride, sodium dihydrogen phosphate and potassium chloride of analytical grade were purchased from Himedia, India. Cysteamine hydrochloride (Cyst) was purchased

CREATED USING THE RSC ARTICLE TEMPLATE (VER. 3.1) - SEE WWW.RSC.ORG/ELECTRONICFILES FOR DETAILS

Analyst www.rsc.org/xxxxxx | PAPER

from Sisco research laboratory, India. 1, 2-dioleoyltrimethylammoniumpropane (DOTAP) and ethidium bromide (EtBr) were purchased from Sigma-Aldrich, USA. Deionized water (DI) was used for preparing all experimental solutions. Thiolated capture probe (I), complementary (II), non-complementary (III) and single nucleotide polymorphism (SNP) (IV) target sequences were all synthesized by MWG biotech, Ebersberg, Germany, with HPLC purification and the sequences are as reported previously.[77] They are HS-$(CH_2)_6$-TAT TAA CTT TAC TCC-3‘, 5‘-CTT CCT CCC CGC TGA-3’ (I), 5’-TCA GCG GGG AGG AAG GGA GTA AAG TTA ATA-3’ (II), 5’-CTG GGG TGA AGT CGT AAC AAG GTA ACC GTA GGG GAA C-3’(III), 5’-TCA GCG GGG AGG ACG GGA GTA AAG TTA ATA-3’(IV), respectively.

Instruments

A conventional three electrode cell consisting of a saturated calomel reference electrode, a Pt wire counter electrode and 2 mm diameter Au disk working electrode having 0.03 cm^2 geometric area was used for all electrochemical measurements. The Au electrode was initially treated with piranha solution for ~2-12 hours, and rinsed thoroughly with distilled water. The electrode was then polished using Al_2O_3 powders (5.0, 1.0 and 0.05 µm), sonicated in DI water and potential cycled in 1 M H_2SO_4 between -300 to 1500 mV at a scan rate 100 mVs^{-1} until a constant current behavior was observed.[78] CV and EIS were performed using a 6500D electrochemical analyzer from CH Instruments, Texas, USA, in presence of 1 mM K_3 [Fe (CN) $_6$]/ K_4 [Fe (CN) $_6$] (1:1) in PBS buffer (pH 7.4). The CV was recorded in the potential window −200 to +700 mV at a scan rate 50 mVs^{-1}. The EIS measurements were made by applying an ac potential amplitude ±5 mV over the dc potential 250 mV (redox potential of K_3 [Fe (CN) $_6$]/ K_4 [Fe (CN) $_6$] (1:1) in PBS) in the frequency range 100 kHz - 1 Hz. Impedance data were plotted in the form of Nyquist plot. Zsimpwin software was used to determine the charge transfer resistance (R_{CT}), double layer capacitance interms of constant Phase element (Q_{CPE}), and contributions from the monolayers. FTIR spectra were recorded using Perkin Elmer Nicolet IS10 in the frequency range 4000–400 cm^{-1}. AFM images in non-contact mode were acquired using Veeco dicaliber High Value Scanning Probe Microscope, USA and silicon nitride RTESP tip. UV-visible spectra were recorded using Shimadzu UV2450 high-performance single monochromator instrument in the frequency range 400–700 nm. TEM images were obtained using Tecnai $G^2$20 instrument from FEI Company, Hillsboro, USA. Dynamic light scattering with zeta potential measurements were made using Horiba nano particle size analyzer, Model SZ-100, which uses green laser light of wavelength 532 nm.

DOTAP–AuNP nano composite preparation, immobilization on cysteamine layer and DNA hybridization

The commercial DOTAP lipid is diluted in chloroform and stored at -20 ^{0}C as stock solution. 1 mM DOTAP lipid was prepared in chloroform, allowed to dry, rehydrated in buffer (pH 7.4) for three times and sonicated for 15 minutes. Water bath sonicator was used to avoid the titanium metal contamination by probe sonicator tip.[79-81] The AuNPs were prepared by Frens method[82,83] using sodium citrate. The hydrated DOTAP and AuNP solutions were mixed at 1:1 ratio and sonicated for 10 minutes just before the experiment. For immobilization of the DOTAP-AuNP nano particles onto the electrode surface, the cleaned Au electrode was immersed in 1 mM cysteamine for 1 hour to form monolayer. 12 µl of DOTAP-AuNP mixture prepared above was drop casted on the cysteamine layer and kept for 1 hour at 4 ^{0}C for the attachment of DOTAP-AuNP. For DNA hybridization sensing experiments, the thiolated ssDNA probe (Capture probe-I, 1 µM of 2 µl DNA in 1 M NaCl, pH 7.0) was dropped onto the DOTAP-AuNP layer and incubated for 2 hours under humid condition[84-86] and washed using the blank PBS buffer to remove the non-reacted ssDNAs. 1 µM of 2 µl target DNA (either II, III or IV) in 4 × SSC buffer was hybridized for 2 hours on different ssDNA surfaces (prepared for each target reactions on an individual electrode surfaces) under identical

experimental conditions. After the target experiment, the dsDNA is de-hybridized using 0.5 M NaOH and washed with PBS buffer to remove the de-hybridized target DNA strands. Subsequently, the non-complimentary target DNA (target probe III) was added onto the de-hybridized surface. The CV and EIS measurements were made intermitantly in presence of $[Fe(CN)_6]^{3-/4-}$. For gene transfection, *E.coli* cells were cultured and isolated following the previous report by Chung et al.[87] The DOTAP-AuNP-ssDNA layer is stained with EtBr dye which interacts efficiently with DNA and investigated under CLSM, scheme 1.

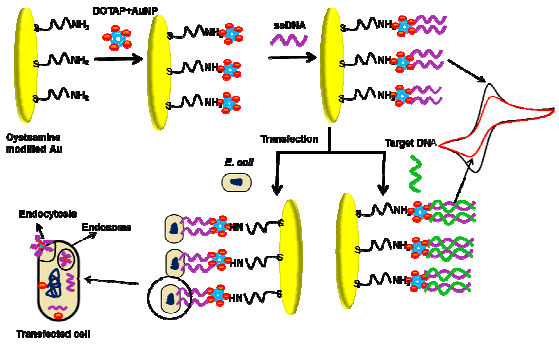

Scheme 1. Tethering of DOTAP-AuNP nano composite on cysteamine monolayer for DNA sensing and transfection using gold transducer

Results and Discussion

Electrochemical behavior of DOTAP-AuNP on cysteamine monolayer on gold electrode

It has been demonstrated that the behavior of liposome-AuNP composites differ in liquid and solid phases and therefore, the electrochemical behaviors of DOTAP and DOTAP-AuNP on gold electrode are examined. Fig.1 shows the CV behaviors of DOTAP (curve b) and DOTAP-AuNP (curve c) layers directly anchored on two different unmodified Au (curve a) electrodes measured in presence of $[Fe(CN)_6]^{3-/4-}$. In agreement with the previous reports,[49-53] the DOTAP insulates the Au surface by forming bilayer indicated by the complete absence of faradaic current for the $[Fe(CN)_6]^{3-/4-}$ redox probe. On the other hand, the DOTAP-AuNP layer showed enhanced redox current, but with ill-defined voltammetric peaks (Fig.1, curve c).

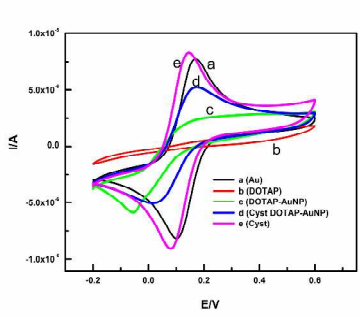

Fig.1. CV behavior of surface modified gold electrode (curve a, unmodified) using DOTAP (curve b), DOTAP-AuNP (curve c), Cysteamine DOTAP-AuNP (curve d) and cysteamine (curve e) monolayers in phosphate buffer (pH 7.4) containing $[Fe(CN)_6]^{3-/4-}$ measured at a scan rate 50 mVs^{-1}.

This is due to the poor control of spherical structured DOTAP-AuNP on the electrode surface. This requires detailed investigation on the interaction and stability of the AuNP camouflaged DOTAP liposome in PBS solution using DLS, UV, FTIR, AFM and TEM techniques. Since DLS gives better insight on the stability of the liposome and lipid-AuNP composites, the DLS studies are made for the AuNP, DOTAP and DOTAP-AuNP in the PBS buffer having ionic strength 0.055M. The average particle sizes of 64, 1715, 14.9 nm with ζ-potentials of -28.0, 7.0 and -0.5 mV, respectively, are observed for the AuNP, DOTAP and DOTAP-AuNP particles.[88,89] The low ζ-potentials for the AuNP (-28 mV) indicate high negative charge density from citrate capping agent, Fig.2. The ζ-potential of 7 mV for the DOTAP suggests the effective stabilization of positive charges by the Cl^- ions in the PBS buffer. It has been shown that cell membranes are surrounded by Na^+, K^+, Ca^{2+}, Mg^{2+}, or Cl^- ions from aqueous buffer with different concentrations inside and outside of the membrane. Electrostatic interactions between these ions and the lipid molecules play crucial role in membrane fusion, phase transitions, or transport across the membrane.[90,91] In this work, the Cl^- ions from PBS buffer strongly interacts with DOTAP which contains positively charged quaternary amine leading to the formation larger complexes with reduced mobility similar to the previous literatures. That is flocculation of lipids with hydration layer allowing rapid formation bulk structures, revealed by larger size of 1715 nm.[92-94] When the DOTAP and AuNP are mixed at

CREATED USING THE RSC ARTICLE TEMPLATE (VER. 3.1) - SEE WWW.RSC.ORG/ELECTRONICFILES FOR DETAILS

Analyst www.rsc.org/xxxxxx | PAPER

1:1 ratio in PBS buffer, the positive charges are neutralized by both AuNP and Cl^- and therefore, the DOTAP-AuNP shows smaller negative ζ-potential of -5 mV [89,92] than the un-complexed AuNP. Cl^- ions may be associated with nitrogen ions similar to the zwitter ionic phosphatidylcholine (PC) lipid layer.[91] Similarly, the size of the AuNP complexed with the DOTAP is also reduced to 14 nm compared to the uncomplexed AuNP that has the size of 64 nm.

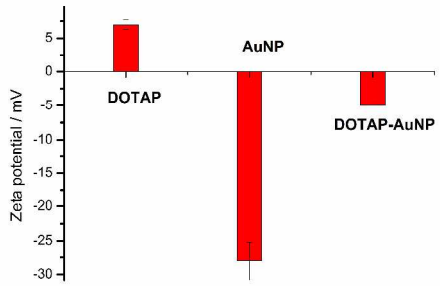

Fig.2. Variation of zeta potential for DOTAP, AuNP and DOTAP-AuNP measured in phosphate buffer (pH 7.4).

The HRTEM of the DOTAP-AuNP Fig. 3B, showed spherical shape with the average size of ~ 50-60 nm confirming the stable spherical nature of the DOTAP-AuNP. The DLS showed a mean size of DOTAP-AuNP is 14.9 in phosphate buffer with the zeta potential of -5.0 mV. The nano particle size differences between the DLS and HRTEM may be related the solution and solid phase measurements. On the solid surfaces the counter ion effects and/or electrostatic interactions between the oppositely charged ions are nullified. Hence, the HRTEM gives highly precized and true size of the dehydrated and shrinked particle size equivalent to the projected area whereas, the DLS give the size corresponding hydrodynamic diameter including the liposome, i.e., hydrated particle size. [95] Collectively these data indicate that the AuNP deposition on the DOTAP arrests the fusion, rapid coagulation and preserve the spherical liposomes which are essential for transfection and other biological applications.[96] The size of DOTAP-AuNP ~50-60 nm (HRTEM, Fig 3B, 4B) from HRTEM and AFM (Fig.4B) confirm the attachment of gold nanoparticle on the DOTAP.

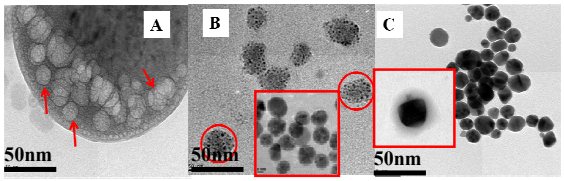

Fig. 3 (A) TEM images of cationic lipid DOTAP (red arrows), (B) DOTAP + AuNP (red circle) and the inset is the HRTEM of AuNP at 5 nm scale and (C) DOTAP + AuNP-DNA Measuring scale bar 50 nm. Optical image of DOTAP is presented in supplementary material, Fig.S8.

Fig. 3A shows the HRTEM of the DOTAP on carbon coated copper grid and the DOTAP has avearge ~ 30-40 nm. The low size reveal the dehyrated DOTAP size again in conflict with DLS data that showed larger size of 1715 nm for the reasons stated above. Again the mean size of 14.9 nm for the DOTAP-AuNP shown by the DLS is smaller than the value observed from HRTEM and the reason for this not known at this time. The 2D AFM images recorded on mica sheet clearly showed circular images for the DOTAP and DOTAP-AuNP, Fig.4A and B. The diameter of the DOTAP-AuNP is upsurged two times than the naive DOTAP due to interaction of AuNP on the head groups of inner and outer layers of the DOTAP bilayer.

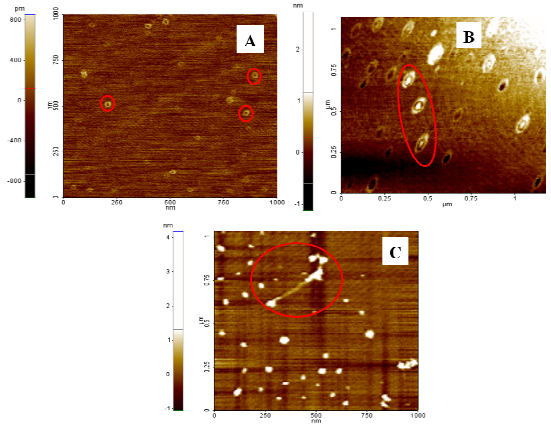

Fig. 4 (A) AFM images of cationic lipid DOTAP, (B) DOTAP + AuNP (red circle) and (C) DOTAP + AuNP-DNA on mica surface

The spherical structure is highly stable on the solid surfaces (carbon copper grid surface used for HRTEM and mica sheets used for

AFM). The size of DOTAP calculated from HRTEM and AFM is ~30-40 nm (Fig 3A, 4A), is 15 times lower than that obtained from DLS (1715.2 nm) due to the solution phase measurement for the reasons stated above. The FTIR showed (Fig. S1) stretching frequencies at 695, 1637, 2070 and 3430 cm^{-1} corresponds to the presence of AuNP. The interaction of DOTAP with AuNP is indicated by the peaks at 2389, 2073 and 1638, respectively, for the CH_2-CH_2 stretching. The decrease of band intensities of the PO_2^- symmetric and asymmetric stretching frequencies after liposome-AuNP formation suggests the prevention of hydrogen bonding between the head groups of DOTAP and AuNPs. The HRTEM image in Fig. 3B shows the presence of AuNP (black dots) on the outer membrane of DOTAP liposome surfaces without disturbing the spherical topography. The AuNP peak intensity at ~520 nm in the UV-visible spectrum is decreased following the interaction with DOTAP, Fig.S2. Hence, direct contact of either DOTAP or DOTAP-AuNP on Au electrode does disturb the spherical ball like structure leading to the formation of bilayer structure preventing the direct charge transfer from $[Fe(CN)_6]^{3-/4-}$, Fig.1, and $[Ru(NH_3)_6]^{3+}$ redox probes, Fig.S3. This necessitates the prevention of direct contact between the electrode surface and liposome. Hence, short chain cysteamine layer[97,98] is used to anchor the DOTAP and DOTAP-AuNP layers. Attachment of DOTAP and DOTAP-AuNP composites on the cysteamine layer increases the redox behavior of $[Fe(CN)_6]^{3-/4-}$ compared to the directly attached DOTAP and DOTAP-AuNP layers on the Au electrode surface. In order to probe the effect of cysteamine layer further, the redox behavior of the cysteamine layer on Au surface is monitored in presence of $[Fe(CN)_6]^{3-/4-}$. It is important to note that the lone cysteamine layer increases the reversibility of the $[Fe(CN)_6]^{3-/4-}$ (increased redox peak currents and decreased peak-to-peak separation (ΔEp) 68 mV than the bare Au electrode (8.72 μA (i_{pa}) and 74 mV (ΔEp)), Fig.1, curve e, due to the catalysis of the negatively charged $[Fe(CN)6]^{3-/4-}$ by the positively charged primary amine head group of the cysteamine.[99-102] Similar behavior is noticed for seven different electrodes prepared under similar experimental conditions and observed the standard deviation for the peak current is 0.97 ± 0.2. Indentical impedance behavior is noticed for the above monolayers, Fig.S4. The impedance data are simulated using the Randles equivalent circuit $[R_S\ (Q_{CPE}(R_{CT}W)(C_L\ R_L)]$.[78] In this circuit R_s solution resistance, Q_{CPE} constant phase element (CPE) representing the capacitance of the Au electrode, R_{CT} charge transfer resistance of Au electrode, W is Warburg element, C_L and R_L are capacitance and resistance of the molecular layer tethered on the surface, respectively. In Fig.S4, the $[R_S\ (Q_{CPE}(R_{CT}W)(C_L\ R_L)]$ circuit fit data is shown for the cysteamine modified Au electrode surface as solid line. The frequency dependent impedance Z (ω) and Q_{CPE} are related by equation $Z(\omega) = 1/Q_{CPE}(j\omega)^n$ $\omega = 2\pi f$ is the angular frequency, in which f is frequency, n is dimensionless CPE exponent indicating the degree of surface roughness and in-homogeneity of the electrode surface which varies between 0 and 1. The CPE exponent 'n' values for cysteamine (0.8 ± 0.1), DOTAP (0.76±0.04) and DOTAP-AuNP (0.71 ±0.02) modified electrodes indicate porous nature of the monolayer structure which constitutes the rough surface. In corroboration with the CV results, the EIS showed decreased and increased R_L values for the cysteamine (31.36 Ω cm^{-2}), DOTAP (116.1 Ω cm^{-2}) and DOTAP-AuNP (93.78 Ω cm^{-2}) monolayers, respectively, Fig.S4. Similarly, the R_L showed a similar trend for the cysteamine (R_L: 2.91×10^4 Ω cm^{-2}), cysteamine-DOTAP (R_L: 2.34×10^5 Ω cm^{-2}) and cysteamine-DOTAP-AuNP (R_L: 3.86×10^5 Ω cm^{-2}) monolayers. Moreover, decreased redox activities for both the $[Fe(CN)_6]^{3-/4-}$, Fig.1, and $[Ru(NH_3)_6]^{3+}$ (Fig.S3) redox probes following the interaction of DOTAP-AuNP indicate decreased charge transfer rate. In contrast, both the redox probe showed enhanced peak currents (increased charge transfer rate) for the pristine cysteamine layer suggesting the catalysis by the primary amine groups.[99-102] Hence, the decrement in the charge transfer rate in presence of DOTAP-AuNP is attributed to surface passivation by

CREATED USING THE RSC ARTICLE TEMPLATE (VER. 3.1) - SEE WWW.RSC.ORG/ELECTRONICFILES FOR DETAILS

the DOTAP-AuNP nano dots on the monolayer. These data indicate the fact that the use of AuNP on the DOTAP head groups plays three different roles in the development of spherical liposomes for electrochemical applications. First, the AuNPs prevent the vesicle fusion of spherical lipids. Second, provide simple method of surface modification and functionalization of liposome by the AuNPs on cysteamine layer through Au-amine linkage. Finally, the presence of AuNP simplifies the biomolecular immobilization chemistry for DNA and other biomolecular sensing or other biological applications.

Because of its simplicity in immobilization chemistry and stability, the thiolated DNA is immobilized onto the DOTAP-AuNP through gold thiol chemistry. The increased intensity of the phosphate asymmetric stretching peak at 1231 cm^{-1} after the DNA interaction with the liposome denotes the efficient interaction between the lipid-AuNP and ssDNA. The amine stretch from thymine is observed at 1271 cm^{-1}.[103] The peak intensities of the DOTAP at 2773, 2669 and 2561 cm^{-1} are decreased following the Au interaction and/or DNA. This is further supported by the decrease of the symmetric and asymmetric $-CH_2$ vibrations profoundly observed for the hydrophobic interaction of DNA. C = O stretching vibration is found in the region 1700-1740 cm^{-1} [104-108] and PO^{2-} stretching at 1222 cm^{-1} is shifted to 1229 cm^{-1}. The peak intensities in the region 2380, 2564, 1230 and 1375 cm^{-1} have been significantly increased signaturing the interaction of DNA with DOTAP-AuNP, Fig.S1. Since the AuNP forms the outer shell to protect the DOTAP core shell, large numbers of HS-ssDNA are immobilized on the DOTAP-AuNP. HRTEM image of the DOTAP-AuNP is increased by 2-5 nm due to the presence of DNA, Fig.3C. The presence of DNA on the DOTAP-AuNP is clearly visible as diffused layer, inset of Fig.3C. The AFM image validated the filamentous DNA which exactly binds on the lipid–AuNP surface, Fig.4C (circled). The DLS showed increased size of ~1203 nm compared to the DOTAP-AuNP that showed 14.9 nm.

Immobilization of thiolated single strand DNA (capture probe I) on the DOTAP-AuNP through thiol-gold chemistry decreases both the anodic and cathodic peak currents (I_{pa} 5.86 from 7.4 µA, i_{pc} -3.36 from -5.022 µA), Fig.S5. and increased the R_L ($5.02\times10^5\ \Omega\ cm^{-2}$ from $1.10\times10^4\ \Omega\ cm^{-2}$), Fig.5. The decreased peak current and increased resistance (R_L) suggests the effective blocking of electrode surface by the negatively charged DNA that exerts high electronegative repulsion for linear diffusion of $[Fe(CN)_6]^{3-/4-}$. Inspite of this, the appearance of sigmoidal CV behavior for both $[Fe(CN)_6]^{3-/4-}$ (with decreased peak current and increased ΔE_p) and $[Ru(NH_3)_6]^{3+}$ (with increased peak currents and decreased ΔE_p) indicate the presence of the pinholes in the monolayer through which the redox probes are accessed. For the DNA hybridization sensing, two different surfaces with similar charateristics are prepared under similar experimental conditions and used for the complementary and non-complementary hybridization experiments. Formation of complementary dsDNA decreases the CV current (3.96 µA) (Fig. S5A, B) and increases the R_L ($91\times10^6\ \Omega\ cm^{-2}$) further. The non-complementary target hybridized (negative control) surface doesn't show any significant changes in the CV and EIS behavior (R_L $4.97\times10^4\ \Omega\ cm^{-2}$ and $3.28\times10^4\ \Omega\ cm^{-2}$), Fig.5, inset. Another experiment using the single nucleotide polymorphism target (probe IV, mismatch indicated by bold and italic character) probe hybridized surface showed an insignificant change in the ΔR_L, Fig.S6.

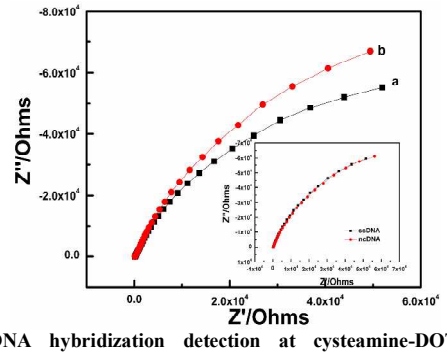

Fig.5. DNA hybridization detection at cysteamine-DOTAP-AuNP modified gold electrode in phosphate buffer pH 7.4. Curve a: Single stranded DNA. Curve b: Double stranded DNA (fully complementary). Non complementary behavior is shown as insert. Impedance data recorded in the frequency range 100 kHz to 1 Hz at an applied potential 250 mV.

Fig.6 showed variation of difference in the charge transfer resistance of the layer ΔR_L (layer resistance difference between the ssDNA and dsDNA surfaces) on effect of changing the target DNA concentrations (curve a obtained for complementary probe II and curve b obtained for non-complementary probe III with respect to capture probe I).

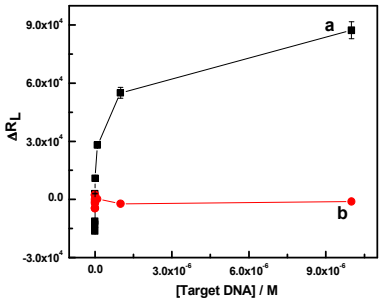

Fig.6. ΔR_L vs. concentration for the complementary (curve a) and non-complementary target DNA concentration in presence of 1 mM $[Fe(CN)_6]^{3-/4-}$

For studying the target DNA concentration effect, the hybridized surface is dehybridized using 0.5 M NaOH and re-hybridized using new target concentrations and the EIS measurements are repeated.[109] The lowest concentration detected is 100 atto molar (1×10^{-16} M). Below this concentration, the surface showed false positive results, even in the low frequency region due to less number of dsDNAs formed on the DOTAP-AuNP surface. Similar experimental observations obtained using the DPV, Fig.S7, confirm the highly stability, sensitivity and selectivity of the spherical DOTAP-AuNP surface on the cysteamine monolayer. The surface is further evaluated for transfection studies using *E. coli* bacterial cells. It may be noted that spherical liposomes constructed using DNA functionalized liposome and stertAvidine-biotin interactions also showed detection limit in 1×10^{-12} M (femto molar) concentration range, however enzyme tags used for enhancing the detection limit .[69] It may be noted that the self-assembled monolayer based DNA sensor on gold transducer reported by Dharuman et al,[75,76] exhibit only picomolar concentration (1×10^{-12} M) detection limit.

Cell transfection

In this study, we have attempted to transfer the DOTAP-AuNP-ssDNA into the *E. coli* cells just by dropping them on the electrode surface. Before dropping the cultured cells, the surface is incubated with EtBr intercalator for staining the dsDNA and washed thoroughly to remove unreacted EtBr. EtBr preferentially binds to the DNA of any given species which is effectively used in transfection studies. [110] Then the cells are dropped and incubated for 1 hour, detached and imaged using CLSM. Fig. 7A indicates the green fluorescent confocal image for the EtBr stained DNA immobilized on DOTAP+AuNP.[111] It is proved that AuNP can stabilize the liposome and DNA and acts as an efficient delivery system. The transfection occurs via endocytosis and transfect the cell,[112] Scheme 1. Fig. 7B shows the DIC image of *E. coli* cells and Fig. 7C shows the DNA transfected *E. coli* cells. The green flourescence inside the cells indicates the incorporation of DNA into the viable *E. coli* cells and some cells are not exhibit fluorescence , indicated by arrows in red, due to the fact that these cells are located far away from the reactive sites on which DOTAP-AuNP-ssDNA are immobilized.

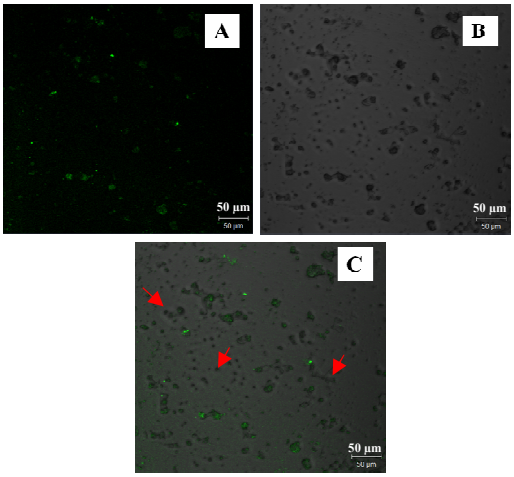

Fig. 7. CLSM images of EtBr stained ssDNA (A), DIC image of *E. coli* (B) and image of DNA transfected *E. coli* cell after transfection on the surface of DOTAP-AuNP-DNA immobilized on cysteamine layer.

Conclusions

We have shown that the spherical structure of liposome was camouflaged with the AuNPs on the cysteamine monolayer modified gold surface by simple electrostatic interaction. The lowest detection limit of 100 aM has been achieved without using enzyme tags. Both development of spherical liposome construction on the gold surface and transfection methods are simple and effective compared to the literature reports. As all experiments are made at pH 7.4 methods like potential stripping and pH change are not required for releasing the AuNP from the electrode surface. However, it may be noted that DNA is immobilized on the AuNPs present on the outer layer of the DOTAP liposome. Hence the interaction of the DNA is direct on the cell surface which could be effective only in bacterial cells. For, mammalian cells these DNA need to be protected. Hence, Future work is directed towards understanding the interaction mechanism on these spherical liposone-AuNP DNA complex on different cells. Further it also essential to understand in more detail on the electronic signal dependence on the solution pH, lipid concentration and cationic (DOTAP) liposome interaction with anionic and neutral lipids in different concentration ratios etc., to develop more sensitive and stable liposome–AuNP composites for the solid supported DNA transfection studies to reduce the cost and time.

Acknowledgements

Dr. V. Dharuman grateful to the Department of Science and Technology (DST, SR/S1/PC-11/2010), New Delhi, Government of India for the project support and M. Bhuvana acknowledges DST for the DST-INSPIRE fellowship (DST-IF- 110327).

References

[1] W. Zhan, A. J. Bard, *Anal. Chem.* 2006, **78,** 726.

[2] M. Ikonen, L. Murtomaki, K. S. Kontturi, *J. Electroanal. Chem.*2007, **602,** 189.

[3] R. R. C. New, *Liposomes: A Practical Approach*; Oxford University Press:Oxford, England, 1990, **1**.

[4] E. Sackmann, In *Structure and Dynamics of Membranes: From Cells to Vesicles Eds.* R. Lipowsky, , E. Sackmann; *Elsevier Science B.V. Amsterdam*, The Netherlands, 1995, **1**, 1.

[5] A.M. Carmona-Ribeiro, *Chem. Soc. Rev.* 2001, **30**, 241.

[6] D. Hellberg, F. Scholz, F.Schauer , W.Weitschies, *Electrochem. Commun.* 2002, **4**, 305.

[7] U. Jakobsen, S. Vogel, *Methods Enzymol*. 2009, **464,** 233.

[8] C. Olbrich, U. Bakowsky, C.M. Lehr, R.H. Mu¨ ller, C. Kneuer, *J. Control. Release* 2001, **77**, 345.

[9] P.L. Felgner, G. Modes, *Nature* 1991, **349,** 351.

[10] O. Le Bihan, Raphae¨ Che`vre, S. Mornet, B. Garnier, B. Pitard, O. Lambert, *Nucl. Acids Res.* 2011, **39,** 1595.

[11] T. Huong, T. Shimanouchi, H. Ishii, H. Umakoshi, R. Kuboi, *J. Coll. Interf. Sci.* 2009, **336,** 902.

[12] G. Z. Hu, D. P. Zhang, W. L. Wu, Z. S. Yang, *Colloids Surf. B.* 2008, **62**, 199.

[13] J. Yan, N. V. Berezhnoy, N. Korolev, C. J. Su, L. Nordenskiöld, *Biochimi. Biophys. Acta* 2012, **1818,** 1794.

[14] C. Yoshina-Ishii, S. G. Boxer, *J. Am. Chem. Soc.* 2003, **125**, 3696.

[15] E. Boukobza, A. Sonnenfeld, G. Haran, *J. Phys. Chem. B* 2001, **105**, 12165.

[16] I. Pfeiffer, F. Höök, *J. Am. Chem. Soc.* 2004, **126,** 10224.

[17] C. Weihl, R.L. Macdonald, M. Stoodley, J. Luders, G. Lin, *Neurosurgery* 1999, **44,** 239.

[18] H .D. Chadwick, M. Kingstone, R. M. Stern, B. J. Cook, P. O'Connor, M. Balfour, S. H.Rosemberg, A. E. Cheng, D.P. Smith, D. M. Meeker, E. W. Geddes, F. W. Alton, *Gene Therapy* 1997, **4,** 937.

[19] J. Zabner, S. H. Cheng, D. Meeker, J. Launspach, R. Balfour, M. A. Perricone, J. E. Morris, J. Marshall, A. Fasbender, A. E. Smith, M. J. Welsh, *J. Clinical. Invest.* 1997, **15**, 1529.

[20] H. Maeda, J. Wu, T. Sawa, Y. Matsumura, K. Hori, *J. Controlled Release* 2000, **65,** 271.

[21] A. Fasbender, J. Marshall, T. O. Moninger, T. Grunst, S. Cheng, M. J. Welsh, *Gene Therapy* 1997, **4,** 716.

[22] E.W.F.W. Alton, P. G. Middleton, N. J. Caplen, S. N. Smith, D. M. Steel, F. M. Munkonge, P. K. Jeffery, D. M. Geddes, S .L. Hart, R. Williamson, K. I. Fasold, A. D. Miller, P. Dickinson, B. J. Stevenson, G. McLachlan, J. R. Dorin, D. J. Porteous, *Nature Genetics* 1993, **5**, 135.

[23]M. R. Almofti, H. Harashima, Y. Shinohara, A. Almofti, Y. Baba, H. Kiwada, *Archives of Biochemistry and Biophysics* 2003, **410**, 246.

[24] N.S. Templeton, D.D. Lasic, P.M. Frederik, H.H. Strey, D.D. Roberts, G.N. Pavlakis, *Nat. Biotechnol.* 15 (1997) 647.

[25] M. I. A. Lam, R. P. Cullis, *Biochimica et Biophysica Acta* 2000,

1463, 279.

[26] F. Liu, H. Qi, L. Huang, D. Liu, *Gene Therapy* 1997**, 4**, 517

[27] S. J. Eastman, C. Siegel, J. Tousignant, A. E. Smith, S. H. Cheng, R. K. Scheule, *Biochimica et Biophysica Acta* 1997, **1325**, 41.

[28] C. Kneuer, M. Sameti, U. Bakowsky, T. Schiestel, H. Schirra, H. Schmidt, C. M. Lehr, *Bioconjugate Chem.* 2000, **11**, 926.

[29] T. Niidome, K. Nakashima, H. Takahashic*,* Y. Niidomec, *Chem Comm.* 2004, **1,** 1978.

[30] S. Jin, K. Ye, *Biotechnol. Prog.* 2007, **23**, 32-41

[31] E. C. Cho, L. Au, Q. Zhang, Y. Xia, *Small* 2010, **6**, 517.

[32] W. K. Rhim, J. S. Kim, J.-Min Nam, *Small* 2008, **4**, 1651.

[33] M. M. Mady, M. M. Fathy, T. Youssef , W.M. Khalil, *Eur. J. Med.Phys* 2012, **28**, 288.

[34] C. Kojima, Y, Hirano, E. Yuba, A. Harada, K. Kono *Colloids and Surfaces B: Biointerfaces* 2008, **66**, 246.

[35] J. Liu, A. Stace-Naughton, C. Jeffrey Brinker, *Chem. Comm.,* 2009, **5**,100.

[36] B. Wang, L. Zhang, S. C. Bae, S. Granick, *Proc. Natl. Acad. Sci. USA* 2008, **105,** 18171.

[37] L. Zhang, L. Hong, Y. Yu, S. C. Bae, S. Granick, *J. Am. Chem. Soc* 2006, **128,** 9026.

[38] C.A. Keller, B. Kasemo, *Biophysical Journal* 1998, **75,** 1379.

[39] T. M. Winger, P. J. Ludovice, E. L. Chaikof, *Langmuir* 1999, **15,** 3866.

[40] G. Csucs, J. Ramsden, *J. Biochimi. Biophy. Acta* 1998, **1369,** 61.

[41] M. Suwalsky, C. Schneider, H.D. Mansilla, J. Kiwi, *J. Photochem. Photobiol.B.* 2005, **78,** 253.

[42] Z. V. Leonenko, A. Carnini, D. T. Cramb, *J. Biochimi. Biophy. Acta* 2000,**1509,** 131.

[43] A. Eing, A. Janshoff, H. J. Galla, C. Block, C. Steinem, *Chem.bio.chem Eur. J*. 2002, **3**, 190.

[44] M. Tanaka, E. Sackmann, *Nature* 2005, **437,** 656.

[45] M. A. Mintzer, E. E. Simanek, *Chem. Rev.* 2009,**109**, 259.

[46] K. J. Kwak, G. Valincius, W.C. Liao, X. Hu, X. Wen, A. Lee, B. Yu, D. J. Vanderah, W. Lu, J. Lee, *Langmuir* 2010, **26,** 18199.

[47] V. A. Hernandez, F. Scholz, *Israel Journal of Chemistry* 2008, **48,** 169.

[48] E. Reimhult, F. Hook, B. Kasemo, *Langmuir* 2003, **19**, 1681.

[49] D. Hellberg, F. Scholz, F Schauer, W. Weitschies, *Electrochem. Commun.* 2002, **4**, 305.

[50] X. Xiao, G. A. Montano, A. Allen, K. E. Achyuthan, D. R. Wheeler, S. M. Brozik, *Langmuir* 2011, **27**, 9484.

[51] C.A. Keller, B. Kasemo, *Biophys. J.* 1998, **75**, 1397.

[52] J. A. P. Piedade, M. Mano, M. C. Pedroso de Lima, T.S. Oretskaya, A.M. Oliveira-Brett, *J. Electroanal. Chem* 2004, **564**, 25.

[53] E. T. Castellana, P. S. Cremer, *Surf. Sci. Rep* 2006, **61**, 429.

[54]X. Yan , J. Li , H. Möhwald, *Adv. Mater.* 2012, **2,** 1.

[55] X. Yan, Y. Cui, W. Qi, Y. Su, Y. Yang, Q. He, J. Li, *Small* 2008, **10**, 1687

[56] X. Yan, J. Blacklock, J. Li, H. Mo¨ hwald, *ACS Nano*, 2012, **6**, 111.

[57] RicKert, A. Brecht, W. Gopel, *Biosens. Bioelectr.,* 1997, **12,** 567.

[58] S. Morita, M. Nukui, R. Kuboi, *J. Coll. Interf. Sci.* 2006, **298**, 672.

[59] T. H. Vu, T. Shimanouchi, H. Ishii, H. Umakoshi, R. Kuboi, *J. Coll. Interf. Sci.* 2009, **336,** 902.

[60] E. Brianda, V. Humblotb, C.M. Pradierb, B. Kasemoa, S. Svedhema, *Talanta* 2010, **81**, 1153.

[61] A. Kumar, G. M. Whitesides, *Appl. Phys. Lett.* 1993, **63**, 2002.

[62] A. Kumar, G.M. Whitesides, *Science,* 1994, **263**, 60.

[63] A. Kumar, H.A. Biebuyck , G.M. Whitesides, *Langmuir* 1994, **10**, 1498.

[64] H. Y. Shima, S. H. Leea, D. J. Ahn, K.-D. Ahnb, J.-M. Kim, *Mater. Sci.Eng. C* 2004, **24**, 157.

[65] M. Bally, K. Bailey, K. Sugihara, D. Grieshaber, J. Voros, B. Stadler, *Small* 2010, *6,* 2481.

[66] N. Dave, J. Liu, ACS Nano 2011**, 5,** 1304.

[67] Y.C. Ishii, S.G. Boxer. *J. Am. Chem. Soc.* 2003,**125**, 3696.

[68] M. M. Lozano, C. D. Starkel, M. L. Longo, *Langmuir* 2010, **26**, 8517.

[69] F. Patolsky, A. Lichtenstein, I. Willner, *Angew, Chem. Int. Ed.* 2000**, 39,** 940.

[70] L. Alfonta, I. Willner, *Anal. Chem.* 2001,**73**, 5287.

[71] W.C. Liao, J.A. Ho, *Anal. Chem.* 2009, **81**, 2470.

[72] K.Y.C. Torres, J. Wu, C. Clawson, M. Galik, A. Walter, G.U. Flechsig, E. Bakker, L. Zhang, J. Wang, *Analyst* 2010, **135,** 1618.

[73] P. A. E. Piunno, U. J. Krull, R. H. E. Hudson, M. J. Damha, H. Cohen, *Anal. Chim. Acta* 1994, **288,** 205.

[74] V. Jonsson, *Biotechniques* 1991, **11**, 620.

[75] V. Dharuman, J.H. Hahn, *Biosens. Bioelectron*. 2008, **23**, 1250.

[76] V. Dharuman, B.-Y. Chang, S.-M. Park, J.H. Hahn, *Biosens. Bioelectron*. 2010, **25**, 2129.

[77] Jie Wu, S. Campuzano, C. Halford, D. A. Haake, J. Wang, *Anal. Chem.* 2010**, 82**, 8830.

[78] A.J. Bard, L.R. Faulkner, Electrochemical Methods-Fundamental and Applications, Second Ed. John Wiley & Sons, Inc. 2001, 372.

[79] M.R. Mozafari *Cell. Mol. Biol. Let.* 2005, **10**, 711.

[80] S. Kataria, P. Sandhu A. Bilandi, M,.Akanksha, B. Kapoor, G.L. Seth, S.D. Bihani, Stealth liposomes: a review. *IJRAP* 2011**, 2,** 1534.

[81] M. Riaz, *Pak J. Pharm. Sci.* 1996, **9,** 65.

[82] G. Frens, *Nature* 1973, **241**, 20.

[83] K. J. Kwak, G. Valincius, W.C. Liao, X. Hu, X. Wen, A. Lee, B. Yu, D. J. Vanderah, W. Lu, J. Lee, *Langmuir* 2010, **26,** 18199.

[84] A.B. Steel, T. M. Herne, R. Levicky, M. J. Tarlov, *Biophysical Journal* 2000, **79,** 975.

[85] K. Jayakumar , R. Rajesh, V. Dharuman, R. Venkatasan, J.H. Hahn, S. Karutha Pandian *Biosens. Bioelectr.* 2012, **31**, 406.

[86] V. Dharuman, K. Vijayaraj, S. Radhakrishnan, T. Dinakaran, J. Shankara Narayanan, M. Bhuvana, J. Wilson, *Electrochim. Acta* 2011, **56**, 8147.

[87] C.T. Chung, S.L. Niemela, R.H. Miller, *Proc.Nat. Acad. Sci.USA* 1989, **86**, 2172.

[88] L. Zhang, L. Hong, Y. Yu, S. Chul Bae, S. Granick *J. Am. Chem. Soc*. 2006, **128,** 9026.

[89] B. Wang, J. Zhou, S. Cui, B. Yang, Y. Zaho, B. Zaho, Y. Duan, S. Zhang, *Afr. J. Biotech*. 2012, **11,** 2763.

[90] R. A. Bockmann, A. Hac, T. Heimburg, H. Grubmu¨ ller, *Biophysical Journal* 2003, **85,** 1647

[91] A. A. Gurtovenko, M. Patra, M. Karttunen, I. Vattulainen, *Biophysical Journal* 2004, **86,** 3461.

[92] K. Makino, K., S. Kim, H. Shinagawa, M. Amemura, A. Nakata *J.Bacteriol.* 1991, **173**, 2665.

[93] W.C. Liao, Ja-an Annie Ho**,** *Anal. Chem.* 2009**, 81***,* 2470.

[94] M.U. Trinh, J. Ralston, D. Fornasiero, *Coll. Surf. B: Biointerf.* 2008, **67** 85.

[95] T. Ito, L. Sun, M. A. Bevan, R. M. Crooks, *Langmuir* 2004, **20,** 6940.

[96] L. Zhang, S. Granick, Nano Lett., 2006, **6**, 694.

[97] Z. M, Liu, Y. Yang, H. Wang, Y.-Li Liu, G.-Li Shen, Ru-Qin Yu, *Sens. Actuat. B* 2005, **106**, 394.

[98] Y. Xiao, H.X. Ju, H.Y. Chen, *Anal. Chim. Acta* 1999, **391**, 73.

[99] S.F. Chou , W.L. Hsu, J. M. Hwang, C. Y. Chen, *Analy. Chim. Acta* 2002, **453**, 181.

[100] F. Arduini, S. Guidone, A. Amine, G. Palleschi, D. Moscone, *Sens. Actuat. B* 2013, **179** *, 201.*

[101] Y. Li, S. Wu, Y. Chen, Q. Lu, W. Lun, *Analy. Methods* 2011, **3**, 1399.

[102] D. Erhan, K. Ozer, K.S. Mustafa, A. Cagrı, A. Aylin, *Biosens, Bioelectr.* 2011, **26**, 3806.

[103] S.T. Saito, G. Silva, C. Pungartnik, M. Brendel, *J. Photochem. Photobiol. B: Biology* 2012, **111,** 59.

[104] R.N. Goyal, A. Aliumar, M. Oyama, *J. Electroanal. Chem.* 2009, ***63,*** 1 58.

[105] C.S. Braun, G. S. Jas, S. Choosakoonkriang, G. S. Koe, J. G. Smith, C. R. Middaugh, *Biophysical Journal* ,**84**, 1114.

[106] E. Taillandier, J. Liquier, *Methods Enzymol.,* 1992, **211**, 307.

[107] G. I. Dovbeshko, V. I. Chegel, N.Y. Gridina, O.P. Shishov, Y.M. Tryndiak, V.P. Todor, G. I. Solyanik, *Biospectroscopy* 2002, **67**, 470.

[108] V.V. Andrushchenko, Z. Leonenko, H. van de Sande, H. Wieser, *Biopolymers* 2002, **61**, 243.

[109] D.M. Loprete, K.A. Hartman, *Biochemistry* 199, **32**, 4077.

[110] J. Kapuscinski, *Biotechnic Histochemistry* 1995, **70,** 220.

[111] D. Pornpattananangkul, S. Olson, S. Aryal, M. Sartor, C. M. Huang, K. Vecchio, L. Zhang, *ACS Nano* 2010, **4,** 1935.

[112] R. K DeLong, C. M Reynolds, Y. Malcolm, A. Schaeffer, T. Severs, A. Wanekaya*, Nanotech. Sci. Appl.* 2010, **3**, 53.

Received: ((will be filled in by the editorial staff))
Revised: ((will be filled in by the editorial staff))
Published online: ((will be filled in by the editorial staff))

Analyst

Cite this: DOI: 10.1039/c0xx00000x

www.rsc.org/xxxxxx

RSC Publishing

Tethering of spherical DOTAP liposome gold nanoparticles on cysteamine monolayer for sensitive label free electrochemical detection of DNA and transfection

Mohanlal Bhuvana and Venkataraman Dharuman

Graphical Abstract

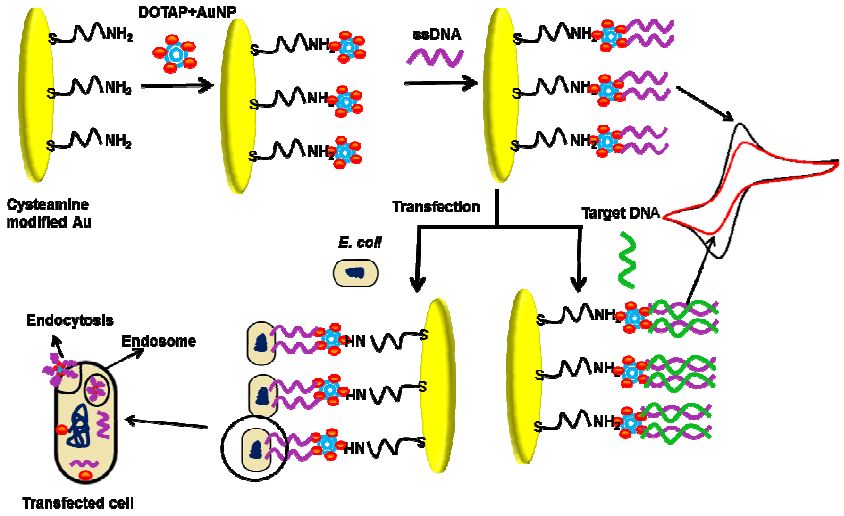

Highlight:

Cysteamine monolayer supported spherical DOTAP-AuNP on gold electrode is developed for DNA label free sensing and transfection